

Mediterranean Forests in Transition (MEDIT): Deliverable No3

Title: Report on the development/structure/validation of the GREFOS v2 model

Due to Project Month 12, Date: 31/03/2013

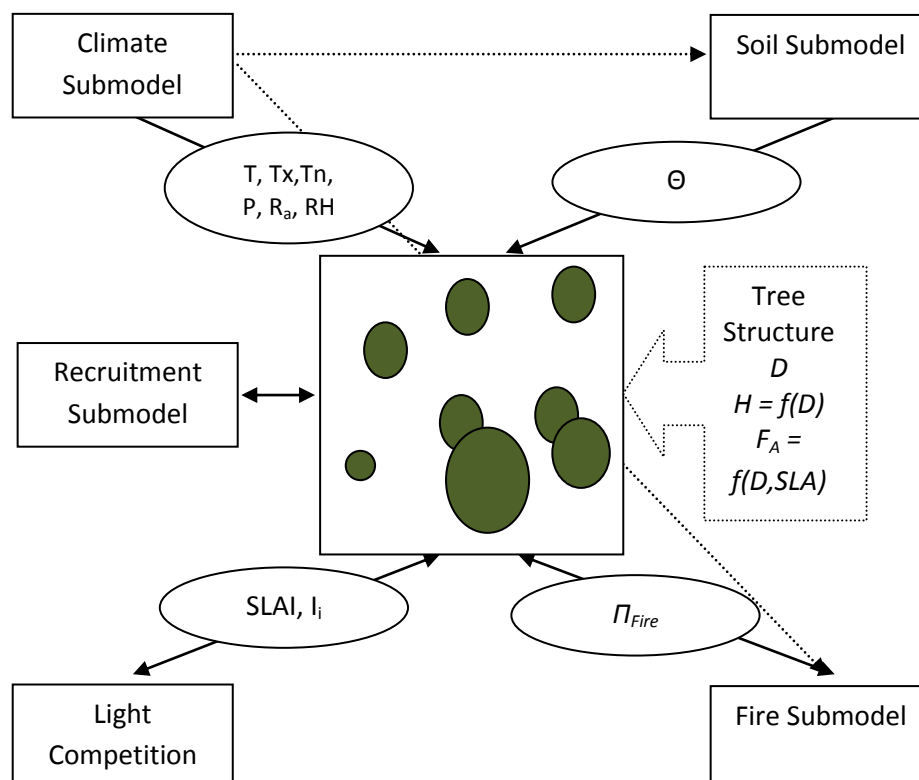
Introduction

This manuscript presents the forest dynamics simulation model GREFOS v2. The original version of the model is a descendant of ForClim (Bugmann and Cramer, 1998; Fyllas et al. 2007). GREFOS v2 builds upon developments of an earlier version of the model (Fyllas & Troumbis 2009) in addition to the detailed regeneration algorithm described in Fyllas et al. 2010. It is a model developed to simulate the dynamics of Mountainous Mediterranean Forest and it specifically parameterised for the dominant tree species found in Greece and the eastern part of the Mediterranean Basin.

GREFOS is a forest gap dynamics simulator (Botkin et al. 1972; Shugart 1984) and it can be broadly categorised as an individual-based model (). It simulates the life cycle of each tree in a small stand (usually 900m²: 30x30m) from its birth to its death. Special interest is given to processes of particular importance like regeneration and growth, and a number of field and laboratory studies have been specifically designed and used to constrain these model components (Fyllas et al. 2008, Fyllas et al. 2010, Galanidis et al. 2013, Fyllas et al. 2013).

The new version of the model has been coded in Java and it is available on request from the author. The following section describes the key model components as summarised in Fig. 1.

Figure 1: Schematic representation of the key model components and their interactions



Model Components

Definition of individual trees

Trees in GREFOS are defined with a diameter based allometry. From the diameter of a tree a set of architectural parameters is estimated using published equations (Gracia et al 1992, Risch et al. 2005). In particular given the diameter at breast height (D) the following individual tree characteristics are defined:

Tree height (H : in cm) is given from:

$H = 130 + b \cdot [1 - \exp(-c \cdot D)]$ (1), with b and c species specific allometric parameters (Fyllas and Troumbis 2009).

The foliage area (FA : in m^2) of a tree is calculated as:

$FA = SLA \cdot \Phi_A \cdot (D^{\Phi_B})$ (2), with Φ_A and Φ_B species specific allometric parameters and SLA the specific leaf area ($cm^2 g^{-1}$) of the species.

The foliage of a tree is assumed to be found at the top (i.e. at height H) defining a circle (flat top canopy)

Climate Submodel

GREFOS simulates climatic processes on a daily timestep. There are two different ways the daily patterns of temperature (T in $^{\circ}C$) and precipitation (P in mm) are generated. The first method reads in daily climate records from local weather stations. The second method uses a built-in weather generator which generates daily values of temperature and precipitation from monthly records, assuming a normal probability distribution for temperature and a log-normal distribution for precipitation (Fyllas & Troumbis, 2009).

Daily extraterrestrial radiation (R_a in $MJ m^{-2} d^{-1}$) is calculated as (Steduto et al. 2009, Raes et al., 2009):

$$R_a = \frac{K_{sc} \cdot dr}{\pi} \cdot [\omega \cdot \sin(\varphi) \cdot \sin(\delta) + \cos(\varphi) \cdot \cos(\delta) \cdot \sin(\omega)] \quad (3)$$

where $K_{sc} = 118.08$ ($MJ m^{-2} d^{-1}$) the solar constant, dr the inverse relative distance between the earth and sun, ω the sunset hour angle, φ the latitude of the plot to simulate and δ the solar declination.

The net shortwave radiation (R_{ns} in $MJ m^{-2} d^{-1}$) is given from:

$$R_{ns} = (1 - \alpha) \cdot R_a \quad (4)$$

where α the canopy albedo taken as constant $\alpha=0.23$.

The net isothermal longwave radiation (R_{nl} in $MJ m^{-2} d^{-1}$) is calculated by a humidity and cloudiness corrected version of the Stefan-Boltzmann law:

$$R_{nl} = f_c \cdot f_h \cdot \sigma \cdot f(T_K) \quad (5)$$

where f_c the cloudiness factor, f_h the air humidity correction factor, σ the Stefan-Boltzmann constant ($4.903 \cdot 10^{-9}$ in $MJm^{-2} K^{-1} d^{-1}$) and

$$f(T_K) = \frac{T_{Kmax}^4 + T_{Kmin}^4}{2} \quad (6)$$

with T_{Kmax} and T_{Kmin} the daily absolute maximum and minimum temperature (K).

The net radiation (R_n) is then calculated as the difference between incoming net shortwave and outgoing longwave radiation:

$$R_n = R_{ns} - R_{nl} \quad (7)$$

The Priestley-Taylor algorithm is used to estimate the daily reference evaporation ET_0 ($\text{MJ m}^{-2} \text{d}^{-1}$):

$$ET_0 = \frac{a_{PT} \cdot s \cdot (R_n - G)}{(s + \gamma)} \quad (8)$$

where a_{PT} the Priestley-Taylor coefficient, s (kPa C^{-1}) the slope of the saturation vapor pressure-temperature relationship, γ (kPa C^{-1}) the psychrometric constant and G ($\text{MJ m}^{-2} \text{d}^{-1}$) the soil heat flux.

Soil Submodel and Water Balance

A single layer soil submodel is used in this version of the model in order to run a daily water balance and estimate a daily soil moisture index (ϑ).

$$\vartheta = \frac{AW}{Z} \quad (9), \text{ with } AW \text{ (mm) the soil available water and } Z \text{ the soil depth (mm).}$$

On a daily timestep AW is computed as:

$$AW_t = AW_{t-1} + P - ET - Q \quad (10)$$

Where ET the actual-stand level evapotranspiration transformed to mm and Q (mm) the soil runoff. A modification to calculate actual evapotranspiration as a function of soil water content has been applied as described in Flint and Childs (1991).

$$ET = a_{sw} \cdot K_c ET_0 \quad (11)$$

Where K_c the crop coefficient [$K_c=0.7$] and a_{sw} the modified Priestley-Taylor coefficient calculated from:

$a_{sw} = A \cdot [1 - \exp(B \cdot \Theta)]$ (12), with $A=0.916$ and $B=-9.74$, and Θ the relative soil water content calculated from (Flint and Childs, 1991):

$$\Theta = \frac{\vartheta - \vartheta_r}{\vartheta_s - \vartheta_r} \quad (13)$$

where ϑ_r the residual soil water content and ϑ_s the water content at saturation. The pedotransfer functions developed in Wösten et al. (1999, 2001) are used to calculate ϑ_r and ϑ_s for the van-Genuchten model, by classifying soils from a coarse to a very fine texture class.

Total stand transpiration (T) and soil evaporation (E_s) are estimated from:

$$T = f_{can} \cdot ET \quad (14),$$

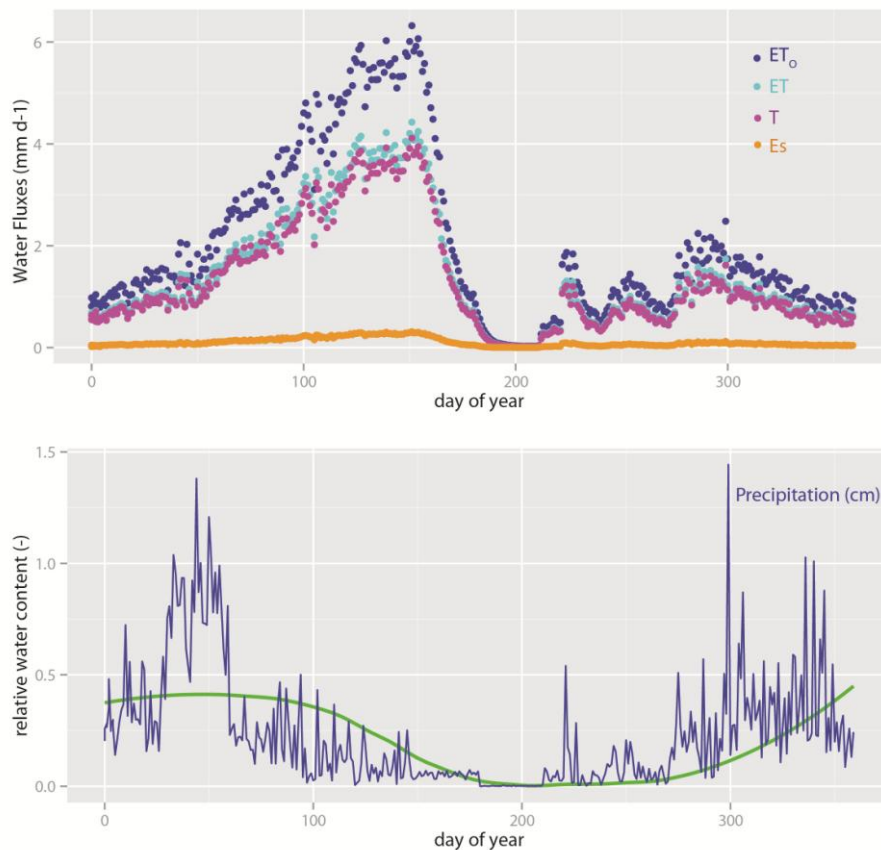
$$E_s = ET - T \quad (15)$$

where f_{can} a correction coefficient for canopy transpiration driven from the stand-level LAI.

$$f_{can} = 1 - \exp(-0.3 \cdot LAI) \quad (16)$$

The modified Priestley-Taylor coefficient (α_{SW}) is used instead of the original α_{PT} in equation 8 to constrain evapotranspiration rates based on the daily soil moisture of the stand. An example of daily water fluxes during a simulation year is given in Fig. 2.

Figure 2: Upper panel: Daily water fluxes in mm d^{-1} at Mt. Parnitha (1300m asl). ET_o the daily potential evapotranspiration of the stand (blue dots), ET the daily actual evapotranspiration (cyan dots), T the daily stand transpiration (magenta dots) and E_s the daily soil evaporation. Lower panel: Relative soil water content (θ) and daily total precipitation over a year.



Recruitment Submodel

In GREFOS special attention has been paid to realistically represent the process of regeneration. To do that we have defined four life history strategies (*LHS*), representing the main strategies followed by typical Mediterranean and mountainous Mediterranean tree taxa (Pausas 1999, Pausas et al. 2004), i.e. seeders (SD), fire seeders (FS), obligate resprouters (OR) and facultative resprouters (FR). Recruitment densities at disturbed (after fire) and undisturbed plots along Greece for each *LHS* have been reported in various studies (Kazanis and Arianoutsou, 2004; Fyllas et al. 2008). The maximum saplings (H: 10-100cm) density for each *LHS* has been used to parameterise the (optimum) recruitment density of the model, as summarised in Table 1.

The optimum recruitment density is subsequently reduced based on two sources of resource limitation for successful regeneration, i.e. light and water availability. Each species is characterised by a threshold of light availability required to achieve a successful establishment of saplings, i.e. the shade tolerance. This species

specific threshold is expressed in GREFOS through a maximum LAI (Leaf Area Index $m^2 m^{-2}$) value above which saplings of a species cannot establish and thus die. Field measurements of recruitment density and survivorship along LAI gradients (Fyllas 2007, Fyllas et al. 2008, Politi et al. 2009) are used to estimate the species specific LAI threshold (LAI_T).

Table 1: Life History Strategies used in Grefos and their associated saplings density

Life History Strategy (LHS)	Maximum Saplings Density (saplings m^{-2})	Typical Species
Fire Seeders (FS)	0.4 // 1.0 (after a fire)	<i>P. halepensis</i> , <i>P. brutia</i>
Seeders (SD)	0.4	<i>A. cephalonica</i> , <i>P. nigra</i>
Facultative Resprouters (FR)	0.3	<i>F. sylvatica</i>
Obligate Resprouters (OR)	0.2	<i>Q. coccifera</i> , <i>Q. frainetto</i>

Recruitment is calculated in GREFOS once a year. The optimum number of new saplings provides a source of new recruits at the age of one year which is added in a pool of available saplings (splPool) for each species. Saplings are maintained in this pool until the age of 10 years, when they are eventually added as trees at a specific location. Until that stage saplings do not have specific coordinates, but are rather considered as a pool of potential recruits. In order for a sapling to increase its age (for example from years 1 to 2) it has to pass the species specific threshold of light availability (LAI_T). At each time step light availability is computed for each member of the saplings pool, by selecting a random location within the plot and estimating a local leaf area index (LAI_L) at a cyclic area of 10 m radius. LAI_L is computed as the sum of foliage area of all established trees within the cyclic area, divided by the area of the circle. No three-dimensional description of the canopy is pursued, and thus if a mature tree falls within the local cyclic area, its entire canopy is assumed to shade the target sapling. This algorithm is essentially “scanning” the forest floor and estimates a level of light availability at random points. If $LAI_L < LAI_T$ then the target sapling survives in the current time step. In contrast, with existing gap models, where an aggregated level of available incoming radiation at the soil surface is estimated, our approach is following a random sampling procedure which could potentially identify more than one gap within the simulated plot area, and thus lead to realistic simulations of areas bigger than the gap scale (Fyllas et al., 2010).

Potential drought effects on saplings survivorship are also taken into account in the new version of the model. A laboratory experiment has been specifically designed for that purpose (Galanidis et al., in prep) where seedlings mortality of representative species has been monitored under discrete drought treatments. A sigmoid curve has been used to fit the mean seedling mortality as a function of the ratio of soil evaporation (E_s) to precipitation reaching the soil (P_s). In the model the amount of precipitation reaching the soil surface (P_s) is considered as a constant fraction (0.76) of daily P (Link et al., 2004). Results from this experimental design are summarised in Fig. 3. These drought mortality functions are used as multipliers of optimum saplings density in the recruitment submodel, to reduce the initial number of saplings to a drought regulated density.

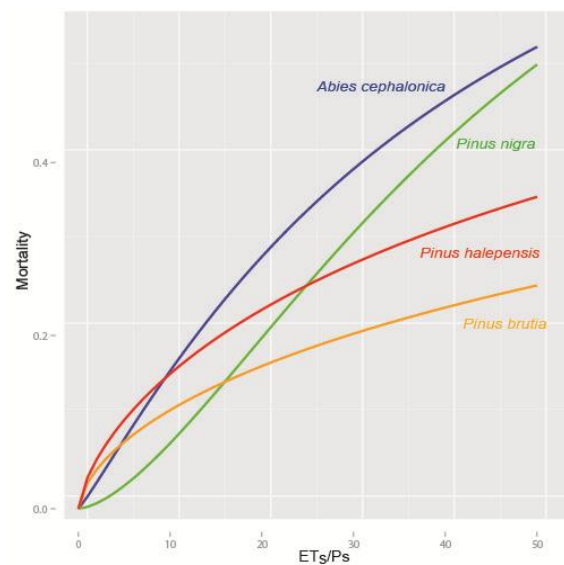


Figure 3: Saplings drought related mortality for four common tree species, as derived from a laboratory experiment specifically designed for that purpose (Galanidis et al., 2013).

Light Competition

Competition for light is the basic competitive process simulated in GREFOS. Two alternative formulations are implemented in the current version of the model.

The first method is the standard light competition algorithm used in forest gap dynamic models, where a competitive hierarchy based on height is assumed (Shugart 1984). Following this algorithm taller trees are assumed to shade all smaller trees and a cumulative shading LAI (SLAI) is estimated for each tree in the stand as:

$$SLAI_i = \frac{1}{A} \sum_{j=1}^{j=m} FA_j \quad (17), \text{ for each tree } i \text{ with } j=1\dots m \text{ all trees with } H_j > H_i$$

The second method follows the Perfect Plasticity model of Purves et al. (2007). Following this formulation trees are characterised as canopy or subcanopy (in or out of canopy). The flat-top version ignores crown depth and assumes that all of a tree's foliage is found at the top of its stem. A canopy height Z^* is estimated for a forest stand defining canopy and subcanopy trees. By summing up the crown area (C_A) of all trees in the stand, Z^* is defined as the height of the last tree that enters to the sum before the cumulative crown area is equal to the plot area.

Results from the first light competition formulation are only presented here.

Growth Submodel

In most forest gap dynamics models the idea of optimum growth curve is used to estimate the annual diameter increment. This algorithm is assuming that for a given size an individual tree of a certain species can achieve an optimum growth, which is then modified by a number of abiotic and biotic factors that represent the non optimum growth conditions in terms of climate and/or competition. In this version of the model, an optimum growth curve has been estimated from annual tree ring width data which are site and species specific. Three environmental factors that reduce optimum growth have been selected, i.e. light availability, heat time (or growing degree days) and water availability.

The optimum growth of an individual (g_o in mm) is described by the equation proposed by Zeide (1993), (see also Fyllas et al., 2012):

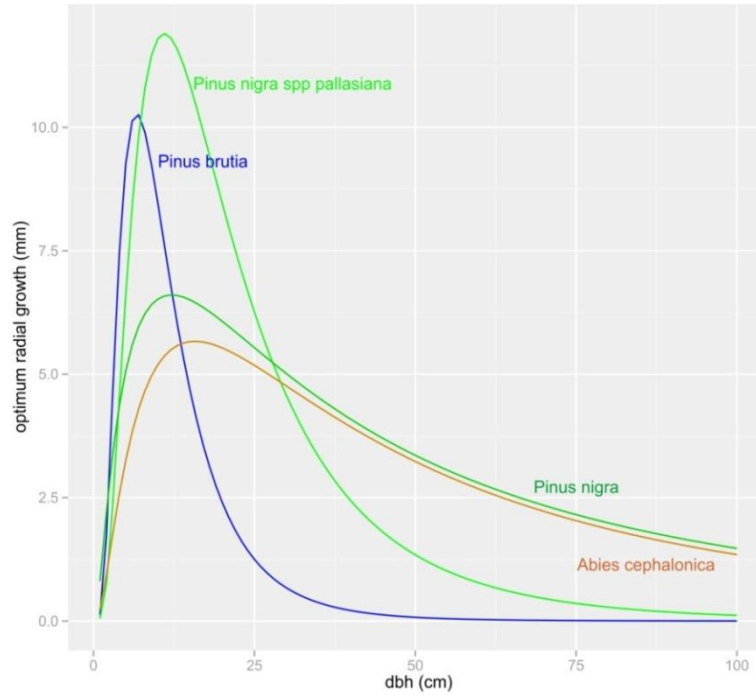
$$g_o = G_m \cdot \exp \left[-0.5 \cdot \left(\frac{\log \left(\frac{D}{D_o} \right)}{D_b} \right)^2 \right] \quad (18)$$

where G_m is the maximum potential growth rate (mm y^{-1}) at the peak of the log-normal growth curve, D_o is the diameter at breast height (D) associated with the maximum growth rate, and D_b determines the breadth of the curve. Tree rings data for a minimum of ten individual trees per species are used to estimate the parameters of equation 18, with a summary of some common tree species given in Table 2. The shape of the optimum growth curve is illustrated in Fig. 4.

Table 2: Optimum growth parameters for some common species in Greece

Species	G_m (mm y^{-1})	D_o (cm)	D_b (-)
<i>Abies cephalonica</i>	11.3	9.12	1.54
<i>Pinus halepensis</i>	17.2	8.90	-1.50
<i>Pinus brutia</i>	19.2	7.09	1.22
<i>Pinus nigra</i>	15.0	6.75	1.61
<i>Quercus ilex</i>	6.0	1.11	1.69
<i>Quercus frainetto</i>	10.7	1.12	2.06

Figure 4: Optimum growth curves for some common tree species



For each tree in the plot an actual growth rate (g_a cm y^{-1}) is subsequently calculated by:

$$g_a = g_o \cdot (LRF \cdot TRF \cdot DRF)^{1/3} \quad (19)$$

where LRF , TRF and DRF the light, temperature and drought response function respectively.

The light response function is given from:

$$LRF = a_1 \{1 - \exp[-a_2 \cdot (I_i - a_3)]\} \quad (20)$$

where I_i is the relative to top canopy available light for tree i , and α_1 , α_2 and α_3 species specific parameters as in Mailly et al. (2000), which define five shade tolerance classes (Fig. 5).

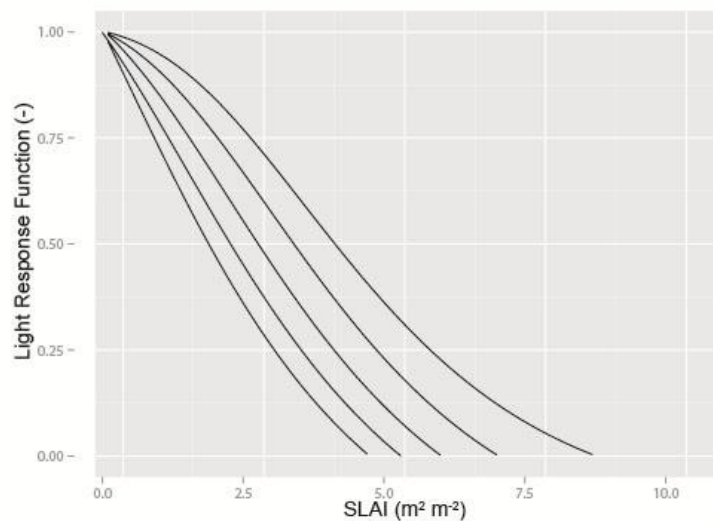


Figure 5: Light response function for the five shade tolerance classes

The temperature response function used in GREFOS v1 (Fyllas et al., 2007) and parameterised for the dominant woody taxa in Greece is also used here:

$$TRF = 1 - \exp[q \cdot (GDD_{\min} - GDD)] \quad (21)$$

Where q is a constant coefficient ($q=0.0013$) and GDD_{\min} a species specific threshold of minimum heat time requirements. GDD is defined as the annual sum of growing degree days with a temperature base of 5 °C.

The original drought response function has been re-parameterised in the current version of the model. Based on the soil water balance algorithm (equations 10 & 13), drought days are defined as those days where $\Theta < 0.1$. A daily drought index (DI) is then estimated as $DI_i = 1 - \Theta_i$, while over the course of a year the annual DI is calculated from the sum of daily DI_i . The response function of six drought tolerance classes is given from:

$$DRF = 1 - \delta \cdot DI \quad (22)$$

where δ a tolerance class specific coefficient ranging from 0.012 for class 1, 0.0084 for class 2, 0.0073 for class 3, 0.0063 for class 4, 0.0055 for class 5 and 0.0047 for class 6.

Mortality Submodel

Three sources of mortality are considered in GREFOS (Fyllas et al. 2007). The *intrinsic or maximum age-dependent* mortality (Π_{im}) assumes that only 2% of a species population reaches its maximum age (Keane et al., 2001) and it is estimated annually for each tree in the stand from:

$$\Pi_{im} = 1 - \exp\left(\frac{-4.605}{Age_{\max}}\right) \quad (23), \text{ where } Age_{\max} \text{ the species specific maximum age.}$$

The *growth-dependent mortality* (Π_{gm}) applies to trees that are not able to achieve an adequate growth for two consecutive years (Solomon 1986, Bigler & Bugmann 2004). These trees are assumed to have a lower survival probability with $\Pi_{gm} = 0.632$. The threshold for adequate growth is set here as the 10% of the optimum radial growth that a tree of a certain species and size would achieve, i.e. $g_a < 0.1g_o$.

The *disturbance-dependent mortality* (Π_{dm}) is linked with the LHS of a tree and takes place only when the stand burns. Species belonging to the seeder (SD) and fire seeder (FS) group are assumed to completely burn and thus $\Pi_{dm}=1$ after a fire event. Facultative resprouters (FR) have a small probability of resprouting and thus for individuals of this group $\Pi_{dm}=0.8$ after a fire. Obligative resprouters (OR) have a higher survival probability and thus in this case $\Pi_{dm}=0.3$.

Fire Submodel

A fire probability is estimated on a daily basis based on the prevailing weather conditions, the structure of the stand and the moisture content of the fuel. The moisture content of the fuel (FMC) is estimated from the empirical equation given in Sharples et al. (2009):

$$FMC = 10 - 0.25 \cdot (T - RH) \quad (24) \text{ where } T \text{ the daily mean temperature (}^\circ\text{C)} \text{ and } RH \text{ the relative humidity of the air (\%).}$$

Fuel moisture of extinction (ME), i.e. the fuel moisture content above which a fire cannot be sustained, is estimated based on the relative contribution of each species to the overall fuel bed, with each species

characterised by a specific ME (Dimitrakopoulos & Papaioannou 2001, Fyllas et al. 2009). The daily ignition probability is then given (Chuvieco et al. 2004):

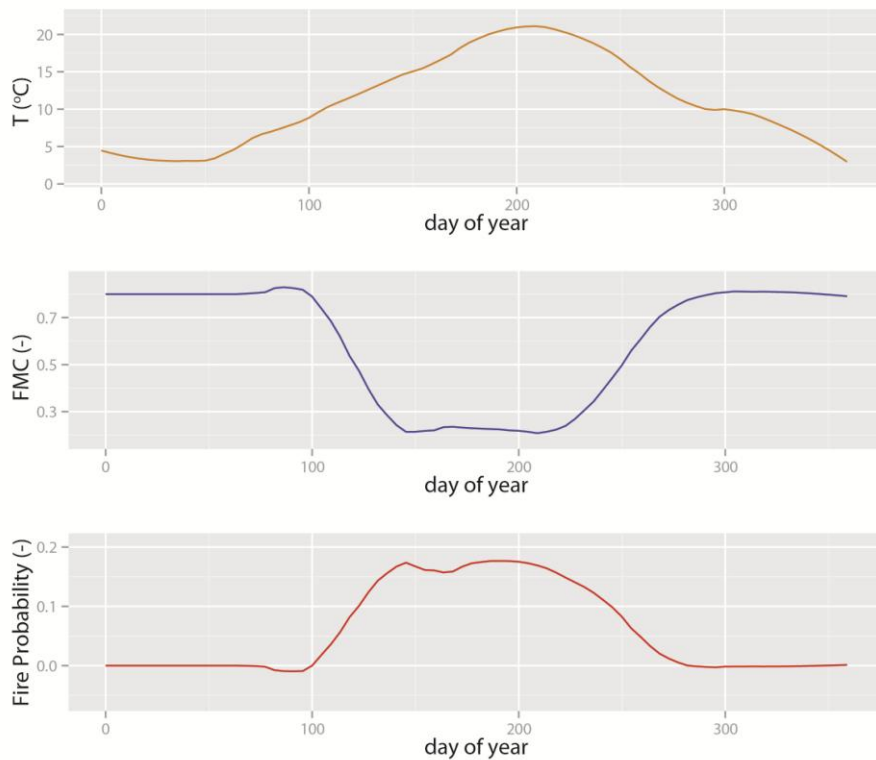
$$\begin{aligned} \text{if } FMC > ME: \quad \Pi_{\text{ign}} &= 0.2 \cdot \left(1 - \frac{FMC - ME}{FMC_{\text{max}} - ME} \right) \\ \text{else: } \quad \Pi_{\text{ign}} &= 0.2 + 0.8 \cdot \frac{ME - FMC}{ME - FMC_{\text{min}}} \end{aligned} \quad (25)$$

with FMC_{max} and FMC_{min} the maximum and minimum FMC values reported in Aguado et al. (2007).

The daily probability of having a crown fire is the estimated assuming that one third of ignitions become crown fires as:

$$\Pi_{\text{Fire}} = \frac{1}{3} \Pi_{\text{ign}} \quad (26)$$

Figure 6: Daily average temperature (T), fuel moisture content (FMC) and fire probability (Π_{Fire}) over the course of a year on Mt Taygetos (1300m asl).

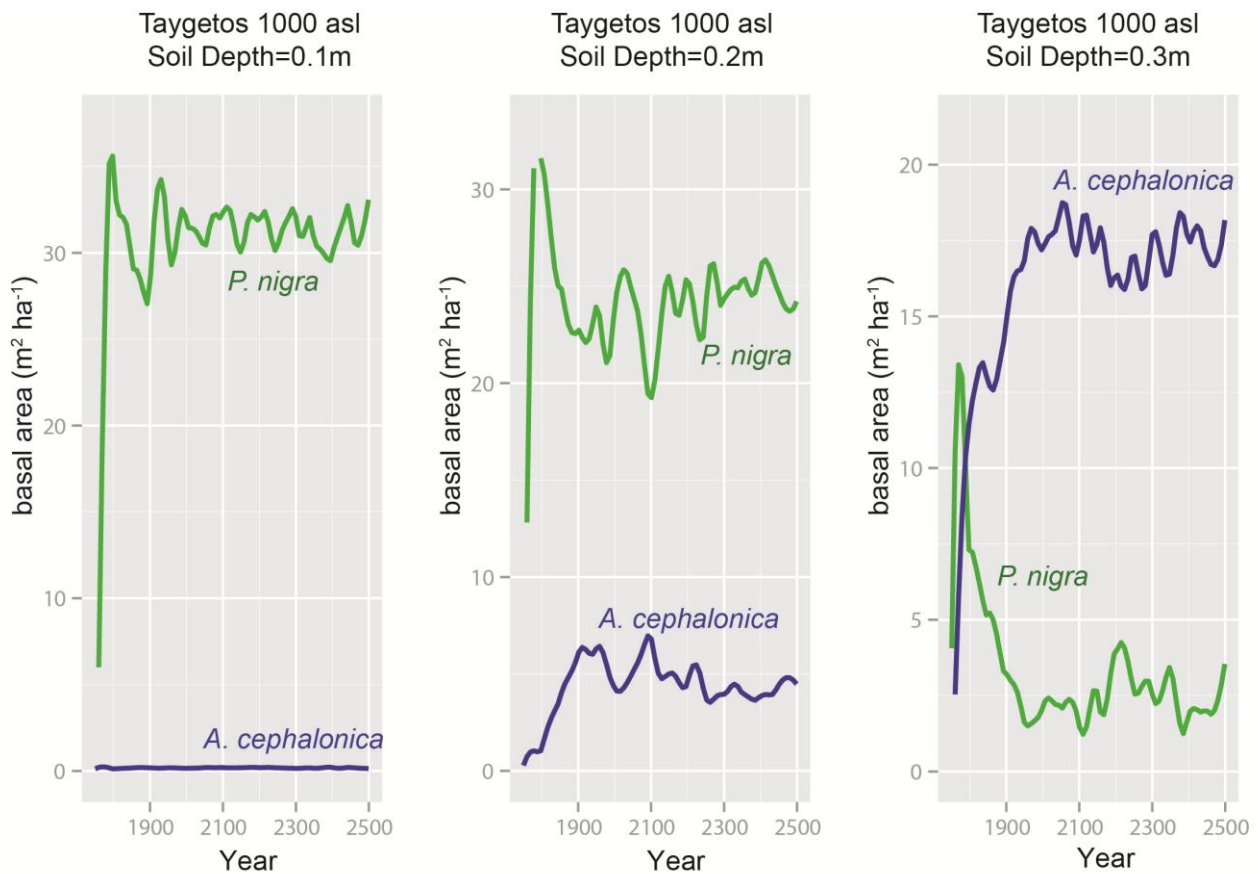


Simulation Exercises

In the following section we provide a set of simulation exercises at three study areas in Greece with contrasting climate patterns. In all study areas the vegetation is dominated by coniferous forest. The dominant species are: *Pinus halepensis*, *Pinus brutia*, *Pinus nigra* and *Abies cephalonica*. Field observations and laboratory experiments are available for the study sites and species of interest. The aim of these simulations is to verify the ability of GREFOS to reconstruct the vegetation patterns and fire regime across the study sites.

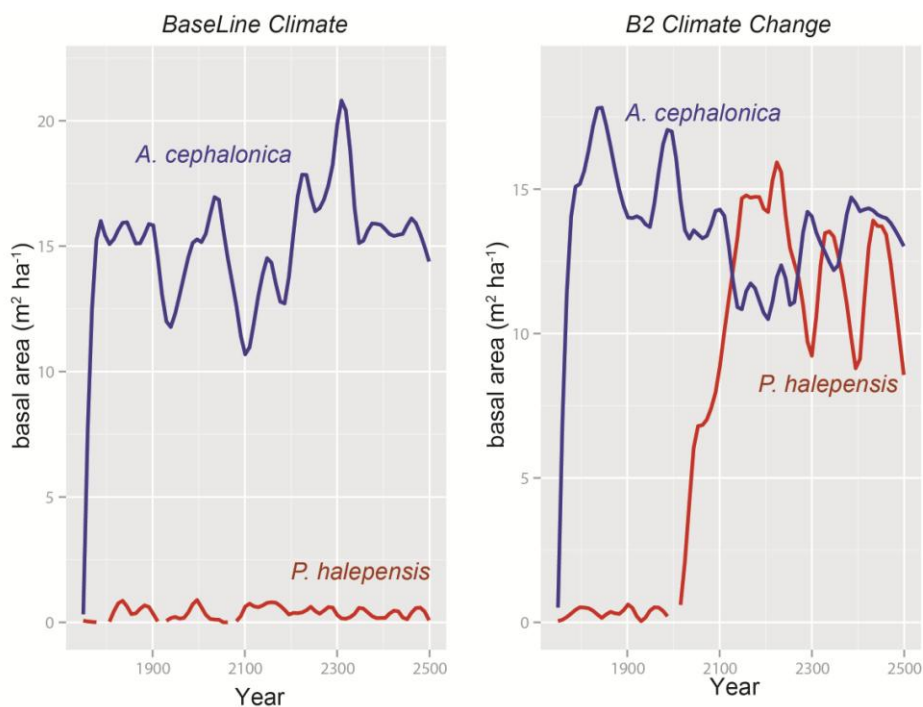
Taygetos *P.nigra* /*A.cephalonica* study site:

Mount Taygetos is found at the southern part of continental Greece. Along a heterogenous landscape with an altitude reaching up to 2400 m asl different forest types are established, but the dominant forest tree species above 600m asl are *P. nigra* and *A. cephalonica*. In general *P. nigra* is more drought tolerant compared to *A. cephalonica* and it is usually found at shallower soils. The ability of the model to shift the vegetation type with changing soil depths was the purpose of the simulation exercise at Mt. Taygetos. Thus at an altitude of 1000 m asl the model was set to run for 750 from bare ground, using again the first 250 years as a "spin-up" period. An additional test of model realism was to compare the simulated MFI with fire-scars data available for the black pine forest in this area (Christopoulou et al. 2013). At shallow soils of 0.1m depth *P. nigra* dominates the stand. With increasing soil depth *A. cephalonica* increases its contribution to the stand biomass, with a complete dominance above soil depths of 0.3m. The MFI ranged from 32 to 34 and to 39 years respectively for increasing soil depth. These estimates were similar to an MFI=30 years measured for this area (Christopoulou et al. 2013).



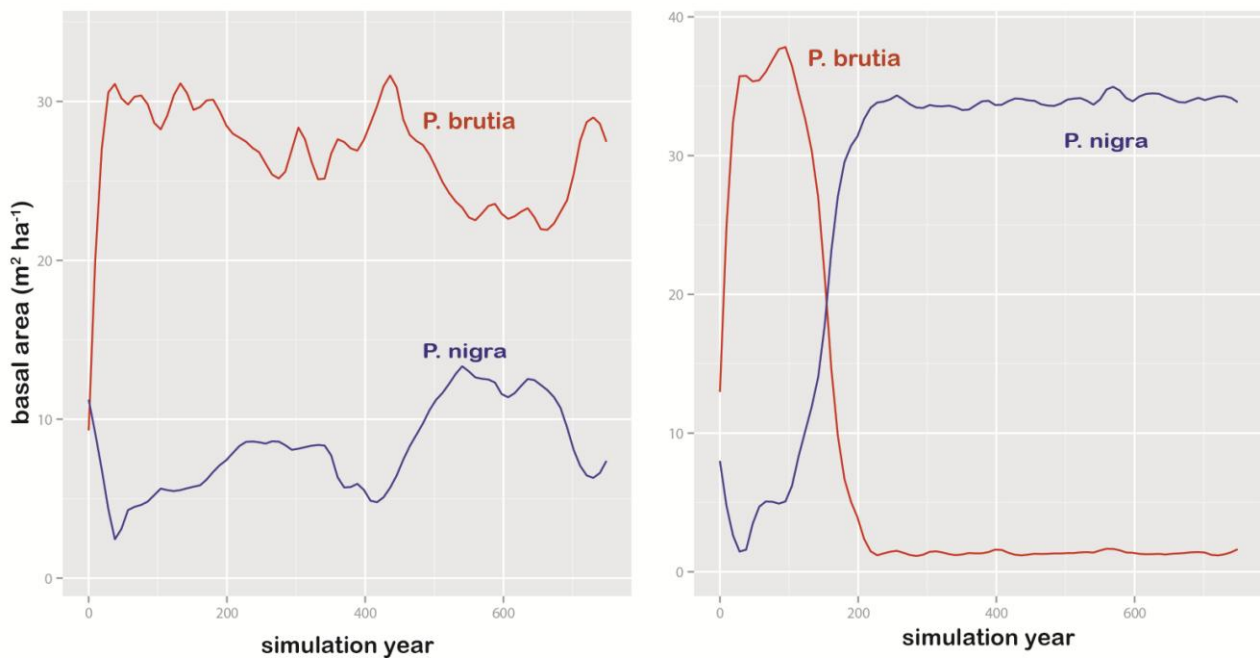
Parnitha P. halepensis / A. cephalonica study site:

At this study area the model was used to explore for potential effects of climatic changes on the dynamics of vegetation. Forest stands at an altitude of 1300m asl, with a soil depth of 0.5m were selected, where currently the endemic Greek fir species (*A. cephalonica*) is the dominant element of vegetation. A comparison between simulations forced with the current climate and a B2 (increase of 2°C in annual temperature and decrease of 5% in precipitation) climate change scenario would highlight potential effects of shifting climate patterns. Under current climatic condition fir dominates the stands with a mean fire return interval of 120 years. However under an increase in temperature and slight decrease in precipitation the model simulates a change in the species synthesis of these stands with a significant increase of *P. halepensis* and a decrease of MFI to 64 years.



Lesbos P. brutia / P. nigra study site:

At this study site a mixed *P. brutia / P. nigra* forest is established at elevations above 600 m asl with unburned northern areas dominated by *P. nigra* (Fyllas et al. 2008). *P. brutia* is a drought tolerant pine adapted to persist to frequent fires through a fire seeding strategy and dominates at low elevation. *P. nigra* is a less drought tolerant pine which forms extensive forest throughout Europe and Greece at the sub-Mediterranean zone. The model was set up to run at an altitude of 700m asl, with a soil depth of 0.5 and a medium soil water holding capacity profile for 750 years. The first 250 years are used a model "spin-up" phase Two simulations experiments were designed ("fire on" and "fire off") to test whether climate or fire is the dominant agent forming the established vegetation patterns. In the first case the model estimated a mean fire return interval (MFI) of 77 years, by fitting a Weibull distribution to the intervals between successive fires (Johnson 1994, Fyllas and Troumbis 2009). In the second case the fire algorithm was turned-off (i.e. $MFI = \infty$) and thus the only source of disturbance driving forest dynamics was gap development. A summary of vegetation development, from bare ground, indicates that the dominance of *P. brutia* and the mixed profile of vegetation at higher altitudes is driven by the local fire regime. Given the local climate profile, exclusion of fire lead to *P. nigra* dominated stands. These simulations are in agreement with field observations from the study site (Fyllas et al. 2008).



References

- Aguado, I., Chuvieco, E., Boren, R., Nieto, H., 2007. Estimation of dead fuel moisture content from meteorological data in Mediterranean areas. Applications in fire danger assessment. *International Journal of Wildland Fire* 16, 390–397.
- Bigler, C., Bugmann, H., 2004. Predicting the time of tree death using dendrochronological data. *Ecological Applications* 14, 902–914.
- Botkin, D.B., Janak, J.F., Wallis, J.R., 1972. Some ecological consequences of a computer model of forest growth. *The Journal of Ecology* 849–872.
- Bugmann, H., Cramer, W., 1998. Improving the behaviour of forest gap models along drought gradients. *Forest Ecology and Management* 103, 247–263.
- Chuvieco, E., Aguado, I., Dimitrakopoulos, A.P., 2004. Conversion of fuel moisture content values to ignition potential for integrated fire danger assessment. *Canadian Journal of Forest Research* 34, 2284–2293.
- Dimitrakopoulos, A.P., 2002. Mediterranean fuel models and potential fire behaviour in Greece. *International Journal of Wildland Fire* 11, 127–130.
- Flint, A.L., Childs, S.W., 1991. Use of the Priestley-Taylor evaporation equation for soil water limited conditions in a small forest clearcut. *Agricultural and Forest Meteorology* 56, 247–260.
- Fyllas, N.M., Dimitrakopoulos, P.G., Troumbis, A.Y., 2008. Regeneration dynamics of a mixed Mediterranean pine forest in the absence of fire. *Forest Ecology and Management* 256, 1552–1559.
- Fyllas, N.M., Phillips, O.L., Kunin, W.E., Matsinos, Y.G., Troumbis, A.I., 2007. Development and parameterization of a general forest gap dynamics simulator for the North-eastern Mediterranean Basin (GREEK Forest Species). *ecological modelling* 204, 439–456.
- Fyllas, N.M., Politi, P.I., Galanidis, A., Dimitrakopoulos, P.G., Arianoutsou, M., 2010. Simulating regeneration and vegetation dynamics in Mediterranean coniferous forests. *Ecological Modelling* 221, 1494–1504.

- Fyllas, N.M., Troumbis, A.Y., 2009. Simulating vegetation shifts in north-eastern Mediterranean mountain forests under climatic change scenarios. *Global Ecology and Biogeography* 18, 64–77.
- Gracia, C.A., Tello, E., Sabaté, S., Bellot, J., 1999. GOTILWA: An integrated model of water dynamics and forest growth, in: *Ecology of Mediterranean Evergreen Oak Forests*. Springer, pp. 163–179.
- Hsiao, T.C., Heng, L., Steduto, P., Rojas-Lara, B., Raes, D., Fereres, E., 2009. AquaCrop—The FAO crop model to simulate yield response to water: III. Parameterization and testing for maize. *Agronomy Journal* 101, 448–459.
- Kazanis, D., Arianoutsou, M., 1996. Vegetation composition in a post-fire successional gradient of *Pinus halepensis* forests in Attica, Greece. *International Journal of Wildland Fire* 6, 83–91.
- Mailly, D., Kimmins, J.P., Busing, R.T., 2000. Disturbance and succession in a coniferous forest of northwestern North America: simulations with DRYADES, a spatial gap model. *Ecological Modelling* 127, 183–205.
- Pausas, J.G., 1999. Response of plant functional types to changes in the fire regime in Mediterranean ecosystems: a simulation approach. *Journal of Vegetation Science* 10, 717–722.
- Pausas, J.G., Bradstock, R.A., Keith, D.A., Keeley, J.E., 2004. Plant functional traits in relation to fire in crown-fire ecosystems. *Ecology* 85, 1085–1100.
- Politi, P.I., Arianoutsou, M., Stamou, G.P., 2009. Patterns of *Abies cephalonica* seedling recruitment in Mount Aenos National Park, Cephalonia, Greece. *Forest Ecology and Management* 258, 1129–1136.
- Purves, D.W., Lichstein, J.W., Pacala, S.W., 2007. Crown plasticity and competition for canopy space: a new spatially implicit model parameterized for 250 North American tree species. *PLoS One* 2, e870.
- Risch, A.C., Heiri, C., Bugmann, H., 2005. Simulating structural forest patterns with a forest gap model: a model evaluation. *Ecological Modelling* 181, 161–172.
- Sharples, J.J., McRae, R.H.D., Weber, R.O., Gill, A.M., 2009. A simple index for assessing fire danger rating. *Environmental Modelling & Software* 24, 764–774.
- Shugart, H.H., 1984. *A theory of forest dynamics. The ecological implications of forest succession models*. Springer-Verlag.
- Solomon, A.M., 1986. Transient response of forests to CO₂-induced climate change: simulation modeling experiments in eastern North America. *Oecologia* 68, 567–579.
- Steduto, P., Hsiao, T.C., Raes, D., Fereres, E., 2009. AquaCrop—The FAO crop model to simulate yield response to water: I. Concepts and underlying principles. *Agronomy Journal* 101, 426–437.
- Wösten, J.H.M., Lilly, A., Nemes, A., Le Bas, C., 1999. Development and use of a database of hydraulic properties of European soils. *Geoderma* 90, 169–185.
- Wösten, J.H.M., Pachepsky, Y.A., Rawls, W.J., 2001. Pedotransfer functions: bridging the gap between available basic soil data and missing soil hydraulic characteristics. *Journal of Hydrology* 251, 123–150.
- Zeide, B., 1993. Analysis of growth equations. *Forest science* 39, 594–616.